Superconductivity in $Fe_{1.05}Te:O_x$ single crystals

Z. T. Zhang,[1] Z. R. Yang,[1,*] W. J. Lu,[1,†] X. L. Chen,[1] L. Li,[1] Y. P. Sun,[1] C. Y. Xi,[2] L. S. Ling,[2] C. J. Zhang,[2] L. Pi,[3] M. L. Tian,[2] and Y. H. Zhang[2,3]

[1]*Key Laboratory of Materials Physics, Institute of Solid State Physics, Chinese Academy of Sciences, Hefei 230031, People's Republic of China*

[2]*High Magnetic Field Laboratory, Hefei Institutes of Physical Science, Chinese Academy of Sciences, Hefei 230031, People's Republic of China*

[3]*High Magnetic Field Laboratory, University of Science and Technology of China, Hefei 230026, People's Republic of China*

(Received 17 October 2013; revised manuscript received 2 December 2013; published 16 December 2013)

We report the discovery of superconductivity at ~9 K in $Fe_{1.05}Te$ single crystals that have been exposed to air for more than six months. The superconductivity is induced due to the oxygen incorporation and only exists in the surface layer of the samples. Our high-resolution transmission electron microscopy experiments and density functional theory calculations show the oxygen prefers to locate at the interstitial site in the Fe-Te layer. X-ray photoelectron spectra characterize an enhancement of the itinerant character of Fe 3*d* electrons, which may reduce the local moment and hence suppress the long-range antiferromagnetism associated with superexchange interactions. This work suggests the bicollinear antiferromagnetism in $Fe_{1+y}Te$ can be suppressed by oxygen incorporation to induce superconductivity and thus could be considered as the parent phase of the superconductivity.

DOI: 10.1103/PhysRevB.88.214511 PACS number(s): 74.70.Xa, 74.62.Bf, 74.70.Ad

I. INTRODUCTION

Since the discovery of superconductivity in tetragonal FeSe, a great deal of efforts have been devoted to studying the microscopic origin of the antiferromagnetism in parent compound FeTe because it is vital to understand the high-temperature superconductivity in the iron chalcogenides.[1–9] An early density functional theory (DFT) study showed that FeTe and iron pnictides have similar Fermi surface (FS) nesting at (π,π) and therefore might exhibit the same spin-density wave (SDW) antiferromagnetic (AFM) order.[2] However, the expected SDW gap in $Fe_{1+y}Te$ was not observed by angle-resolved photoemission spectroscopy (ARPES), which means that the magnetism arises from other interactions different from the case in the iron pnictides.[3] Consistently, a neutron diffraction study revealed a bicollinear magnetic order in $Fe_{1+y}Te$ instead of the collinear SDW order as in iron pnictides.[4] This kind of bicollinear magnetic order could be effectively described using the Heisenberg model with J_1-J_2-J_3 interactions between the local moments of Fe.[5] Fang *et al*. suggested the spin frustration in $Fe_{1+y}Te_{1-x}Se_x$ increases with Se concentration and results in a large quantum critical region.[6] Nevertheless, Liu *et al*. argued the $(\pi,0)$ magnetic order in $Fe_{1+y}Te$ is associated with weak charge carrier localization due to the excess Fe.[7] DFT study also showed the predicted (π,π) FS nesting in undoped FeTe is changed from (π,π) to $(\pi,0)$ by electron doping of excess Fe, which stabilizes the bicollinear magnetic order.[8] Therefore, whether the magnetic ground state in $Fe_{1+y}Te$ arises from the FS nesting that induces itinerant SDW magnetism as the case in the other iron-based superconductors or from the superexchange interactions between the Fe local spins still remains controversial.

Recently, it was reported that thin films of $Fe_{1+y}Te$ can be made superconducting through tensile stress[10] or oxygen incorporation.[11–16] The superconductivity in tensile stressed $Fe_{1.08}Te$ thin films was attributed to the softening of the structural and AFM transitions.[10] Nie *et al*. believed the change of Fe valence state to mainly 3+ may account for the appearance of superconductivity in oxygen incorporated $Fe_{1+y}Te$ films.[11–13] Si *et al*. argued that the superconductivity in thin films of $Fe_{1.08}Te:O_x$ might arise from the substitution of O for Te.[14] However, Zheng *et al*. found their O-substituted FeTe films were nonsuperconducting.[15] Clearly, the reason why superconductivity was usually observed in these pulsed laser deposited $Fe_{1+y}Te$ thin films is still under debate. Moreover, it is noticed that only thin-film samples of $Fe_{1+y}Te$ can be made superconducting and the attempts trying to induce superconductivity in bulk samples of $Fe_{1+y}Te$ through oxygen incorporation or high-pressure application are both failed.[17,18]

In this paper, we report the discovery of superconductivity in $Fe_{1.05}Te$ single crystals which have been exposed to air for more than six months. It is found that oxygen is incorporated and partially occupies the interstitial site of the Fe-Te layer without changing the crystal symmetry. As revealed by x-ray photoelectron spectroscopy (XPS) spectra, the itinerant character of Fe 3*d* electrons is enhanced for superconducting $Fe_{1.05}Te:O_x$. DFT calculations also indicate the interstitial location of oxygen in the Fe-Te layer. This work indicates that the superconductivity can be directly induced from bicollinear magnetic ordered $Fe_{1+y}Te$ by oxygen incorporation and may shed light on the parent magnetic phase of the superconductivity.

II. EXPERIMENTAL AND CALCULATION DETAILS

Single crystals with nominal compositions FeTe were prepared using the self-flux method.[19] High-purity powders of Fe and Te were mixed and grounded thoroughly in an inert atmosphere and then sealed in an evacuated double-wall quartz tube. The tube was sintered at 950 °C and cooled down slowly at a rate of 2 °C per hour. Obtained single crystals can be easily cleaved with typical dimensions of $1 \times 1 \times 0.2$ mm^3. The chemical compositions of the as-grown single crystals

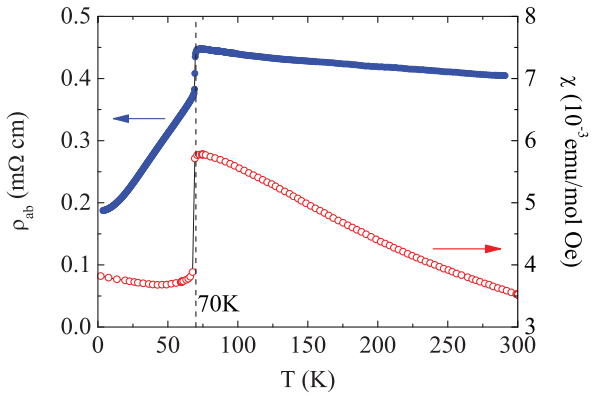

FIG. 1. (Color online) In-plane resistivity ρ_{ab} and magnetic susceptibility χ ($H = 1$ T, $\| c$) as functions of temperature for the as-grown $Fe_{1.05}Te$ single crystal.

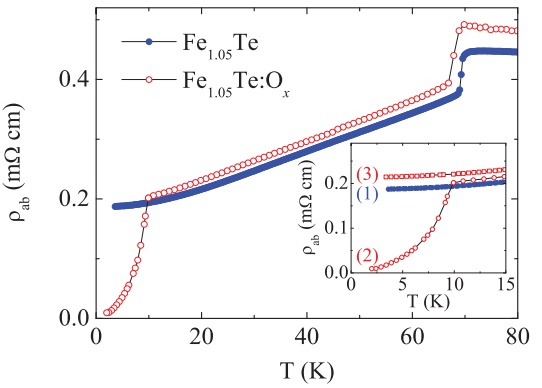

FIG. 2. (Color online) Temperature dependence of ρ_{ab} for $Fe_{1.05}Te$ and $Fe_{1.05}Te:O_x$ single crystals. The inset displays the closeup of ρ_{ab} at low temperatures for (1) $Fe_{1.05}Te$, (2) $Fe_{1.05}Te:O_x$, (3) the surface layer removed $Fe_{1.05}Te:O_x$.

were determined using an energy-dispersive x-ray spectrometer (EDXS). Multiple points measurements indicated an average composition of $Fe_{1.05}Te$, and composition mapping results showed that the spatial distribution of Fe and Te was homogeneous. Some of the $Fe_{1.05}Te$ single crystals are stored in ordinary air atmosphere (pressure ≈1 atm., temperature ≈10 °C–30 °C) for more than six months before their surfaces become superconducting. In-plane resistivity was measured using a standard four-probe method in a Quantum Design Physical Properties Measurement System (PPMS). Magnetic susceptibility was measured using a superconducting quantum interference device (SQUID) magnetometer. High-resolution transmission electron microscopy (TEM) images were taken within the *ac* plane using a JEOL-2010 TEM. XPS experiments were performed under vacuum ($\sim 1 \times 10^{-9}$ mbar) with Al K_α radiation ($h\nu = 1486.6$ eV) using an ESCALAB-250 x-ray photoelectron spectroscope.

The electronic properties were calculated by first principles within DFT. The DFT calculations were performed with the projected augmented-wave (PAW) method[20,21] as implemented in the ABINIT code.[22–24] The exchange-correlation functions are treated by using the generalized gradient approximation (GGA) according to the Perdew-Burke-Ernzerhof[25] (PBE) parametrization. Electronic wave functions are expanded with plane waves up to an energy cutoff (E_{cut}) of 1200 eV. Brillouin zone sampling was performed on a Monkhorst-Pack (MP) mesh[26] of $10 \times 10 \times 12$ for the $2 \times 2 \times 1$ FeTe supercell.

III. RESULTS AND DISCUSSIONS

Figure 1 displays the temperature dependence of in-plane resistivity (ρ_{ab}) and magnetic susceptibility (χ) for the as-grown $Fe_{1.05}Te$ single crystal. The resistivity increases with decreasing temperature from 300 K and shows a sudden drop at $T_N \approx 70$ K. Correspondingly, the susceptibility decreases abruptly at T_N indicating the presence of the structural and AFM transitions, which are in agreement with other groups' reports.[7,9]

After being exposed to air for more than six months, the $Fe_{1.05}Te$ single crystals show the trace of superconductivity. Figure 2 presents the temperature dependence of ρ_{ab} for the superconducting single crystal, which is labeled as $Fe_{1.05}Te:O_x$ (see the composition analysis below). In contrast to $Fe_{1.05}Te$, the ρ_{ab} of $Fe_{1.05}Te:O_x$ exhibits a significant decrease at $T_c^{\text{onset}} \approx 9$ K, characteristic of the appearance of superconductivity. Consistently, the $\chi(T)$ curve displays a superconducting diamagnetic transition at $T_c^{\text{mag}} \approx 8$ K, as is shown in Fig. 3. The superconducting T_c of $Fe_{1.05}Te:O_x$ is very close to those of underdoped $Fe_{1+y}Te_{1-x}Se_x$ and $Fe_{1+y}Te_{1-x}S_x$,[7,19,27,28] indicative of the similarity among them. In Fe_{1+y}(Te,Se/S) superconductors, the long-range AFM order is gradually suppressed by increasing the Se or S concentration.[7,27,28] However, in $Fe_{1.05}Te:O_x$, the AFM transition temperature T_N is not changed compared with that of $Fe_{1.05}Te$. The unchanged T_N is considered to result from the inside of the bulk sample, which implies the superconductivity only exists in the surface layer. In order to approve this deducibility, we remove the surface layer of the $Fe_{1.05}Te:O_x$ single crystal using the scotch-tape method and measure the resistivity on the inside of the sample. As expected, the superconductivity disappears after the surface layer is removed, as shown in the inset of Fig. 2.

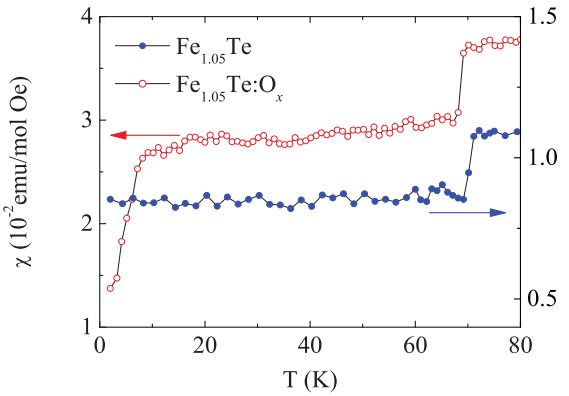

FIG. 3. (Color online) Magnetic susceptibility χ as a function of temperature for $Fe_{1.05}Te$ ($H = 50$ Oe) and $Fe_{1.05}Te:O_x$ ($H = 10$ Oe) with $H \| c$ axis.

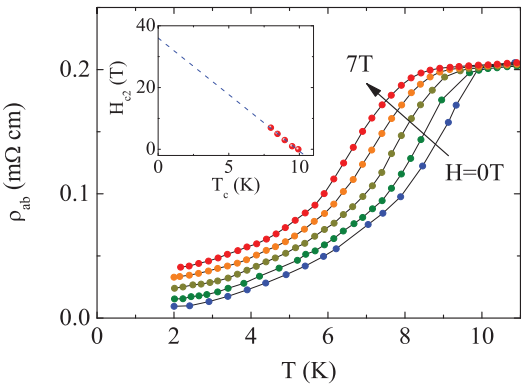

FIG. 4. (Color online) Temperature dependence of ρ_{ab} for $Fe_{1.05}Te:O_x$ measured in the magnetic fields $H = 0$, 1, 3, 5, and 7 T applied along the c axis. The inset is the corresponding upper critical field versus the temperature phase diagram.

The emergence of superconductivity in $Fe_{1.05}Te:O_x$ is further confirmed by resistivity measurements under different magnetic fields. As illustrated in Fig. 4, the T_c^{onset} of $Fe_{1.05}Te:O_x$ decreases gradually with increasing magnetic field up to 7 T as the $H \| c$ axis. The corresponding $H - T$ phase diagram is plotted in the inset of Fig. 4. The slope of the $H_{c2}(T)$ curve, obtained from linear fit, is $dH_{c2}/dT = 3.66$ T/K. Using the Werthamer-Helfand-Hohenberg formula[29] $H_{c2}(0) = -0.693T_c(dH_{c2}/dT)\,|_{T=T_c}$, the upper critical field is estimated as $H_{c2}(0) = 25$ T, a little lower than the 29 T in thin films of $FeTe:O_x$ reported by another group.[16]

To investigate the change of the chemical composition for $Fe_{1.05}Te:O_x$, we performed EDXS measurements on the surface layer of the sample. Only Fe, Te, and O elements are observed by multiple points measurements. The mole ratio of Fe:Te is identical to that of as-grown $Fe_{1.05}Te$, but the O:Te mole ratio varies from 0 to 0.6 indicating the oxygen is distributed inhomogeneously. It is notable that most of the O:Te mole ratio values (from more than 10 region measurements) distribute below 0.2. The spatial scale of inhomogeneity of oxygen distribution might be comparable with that of the intrinsic nanoscale inhomogeneity in Fe_{1+y}(Te,Se/S) materials.[30,31] These results show that the superconductivity in the $Fe_{1.05}Te:O_x$ is associated with the oxygen incorporation.

In $Fe_{1+y}Te$, superconductivity can be induced by isovalent substitution of Se or S for Te.[7,27,28] Therefore, it is natural to question whether the superconductivity in $Fe_{1.05}Te:O_x$ is also due to substitution of O for Te. If so, both a and c lattice parameters would decrease compared with $Fe_{1.05}Te$, just as what happens in $Fe_{1+y}Te_{1-x}Se_x$ or $Fe_{1+y}Te_{1-x}S_x$.[27,28] In fact, the substitution of O for Te has been postulated by Si *et al.* to explain the superconductivity in $Fe_{1.08}Te:O_x$ thin films.[14] But, Zheng *et al.* believed the O substitution for Te is not associated with the superconductivity in oxygen-doped FeTe films.[15] To address this issue, we perform high-resolution TEM measurements on the cross section (i.e., ac plane) of the surface-layer region in $Fe_{1.05}Te$ and $Fe_{1.05}Te:O_x$ single crystals. Figures 5(a) and 5(b) show typical TEM images for both samples. The selected areas' electron diffraction patterns determine the crystal orientation and indicate the

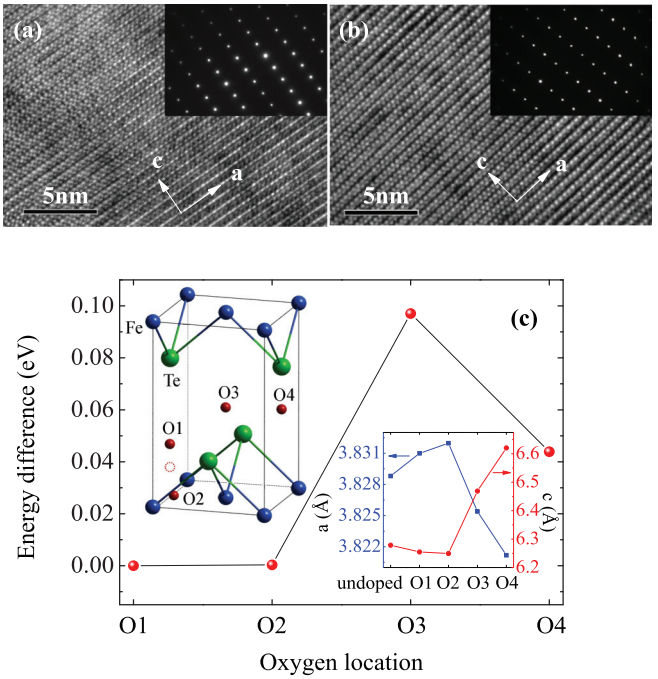

FIG. 5. (Color online) HR-TEM images for (a) $Fe_{1.05}Te$ and (b) $Fe_{1.05}Te:O_x$ recorded within the cross section (i.e., ac plane) of the surface-layer region. The top right insets display the corresponding selected areas' electron diffraction pattern of the samples. (c) Calculated energy difference (in eV per formula unit) for $FeTe:O_{0.125}$ with different oxygen locations. The top left inset shows the four possible symmetric sites for oxygen atoms and the red dotted circle is the final and stable site after full relaxation. For clarity, here only one of the equivalent oxygen atoms for each symmetric site is plotted. The bottom right inset shows the calculated lattice parameters.

crystallographic symmetry of the lattice is not changed by the oxygen incorporation. Large numbers of detailed measurements of the periodicity along the a and c axes on $Fe_{1.05}Te$ show that the average lattice parameters are $a = 3.84$ Å and $c = 6.43$ Å. But, for $Fe_{1.05}Te:O_x$, they are $a = 3.91$ Å and $c = 6.40$ Å, indicating an in-plane expansion and a slight out-plane shrinkage. These results are incompatible with the postulation of O substitution for Te mentioned above. Besides, an intercalation of O between the Fe-Te layers, which would expand the c parameter dramatically, is also not the case for $Fe_{1.05}Te:O_x$. The changes of a and c lattice parameters can be interpreted only if the oxygen occupies an interstitial site in the Fe-Te layer.

In order to simulate the interstitial oxygen, we construct a $2 \times 2 \times 1$ FeTe supercell with one oxygen atom, which corresponds to $FeTe:O_{0.125}$. We consider four cases that the oxygen atom initially locates each of four possible symmetric sites as shown in the top inset of Fig. 5(c). These possible sites were chosen since they have higher symmetry and more space to accommodate excess atoms. The structure relaxation calculations show the oxygen atoms from the initial O1 (in the Te plane) and O2 (in the Fe plane) sites actually relax to almost the same optimal site between Fe and Te planes (notated by a red dotted circle in the figure). This is not strange since

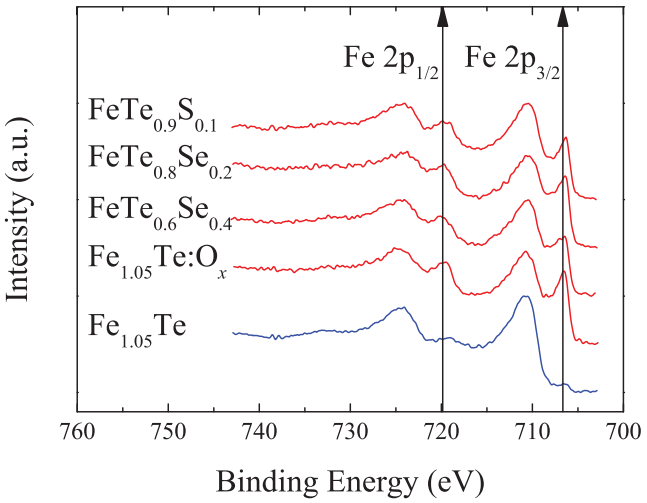

FIG. 6. (Color online) XPS spectra for nonsuperconducting $Fe_{1.05}Te$ and superconducting $Fe_{1.05}Te{:}O_x$, $FeTe_{0.6}Se_{0.4}$, $FeTe_{0.8}Se_{0.2}$, and $FeTe_{0.9}S_{0.1}$ single crystals.

the oxygen tends to bond to both Fe and Te ions. As shown in the main panel of Fig. 5(c), the optimized final structures for cases O1 and O2 have the lowest total energy, indicating the most stable structure. The relaxed structures for cases O3 (body centered) and O4 (face centered) have higher total free energy ($>0.04 \sim 0.10$ eV per formula unit), indicating the unstable structures. In addition, the relaxed lattice parameters for cases O1 and O2 both exhibit a slight expansion in the a axis and a little shrinkage in the c axis compared with those of the undoped FeTe. However, for cases O3 and O4, the relaxed lattice parameter c strongly increases due to the intercalation of oxygen between the Fe-Te layers. Clearly, both the location of oxygen and the change of a and c lattice parameters coincide with the TEM measurements.

Since the interstitial oxygen tends to bond to both Fe and Te ions, it may have significant influence on the electronic property of $Fe_{1.05}Te$ such as the valence state of Fe. Figure 6 shows the XPS spectra of Fe ($2p$) electrons for $Fe_{1.05}Te$ and $Fe_{1.05}Te{:}O_x$. The XPS data of superconducting $FeTe_{0.6}Se_{0.4}$, $FeTe_{0.8}Se_{0.2}$, and $FeTe_{0.9}S_{0.1}$ are also collected for comparison. The peaks at binding energy 706.65 eV ($2p_{3/2}$) and 719.85 eV ($2p_{1/2}$) correspond to Fe^0 as in pure Fe metal,[32–35] and the ones around 710 eV ($2p_{3/2}$) and 723 eV ($2p_{1/2}$) correspond to Fe^{2+} as in $Fe_{1-\delta}O$.[32,36] These peaks indicate a mixed Fe^0/Fe^{2+} valence state in these materials, consistent with the previously reported XPS results in $FeTe_{0.5}Se_{0.5}$.[33] The difference of the spectra for $Fe_{1.05}Te$ and $Fe_{1.05}Te{:}O_x$ mainly comes from the intensity of the Fe^0 peaks. In iron-based superconductors, the presence of the Fe^0 peaks and the absence of satellite peak (712.00 eV) are correlated with the itinerant character of Fe $3d$ electrons.[33–35] For superconducting $Fe_{1.05}Te{:}O_x$, the intensity of the Fe^0 peaks is strengthened compared with that of $Fe_{1.05}Te$. A similar case occurs in the Fe(Te,Se/S) superconductors. Therefore, the emergence of superconductivity as well as the suppression of AFM order in $Fe_{1.05}Te{:}O_x$ and Fe(Te,Se/S) can be correlated to the enhancement of the itinerant character of Fe $3d$ electrons.

We have shown that superconductivity is induced in the $Fe_{1.05}Te$ single crystal by oxygen incorporation, accompanied by the suppression of the AFM ground state. The AFM ground state in $Fe_{1+y}Te$ raises a crucial question for the iron-based superconductors: Do all of them share the same magnetic origin? For the iron pnictides, the FS nesting between the hole and electron pockets leads to a SDW magnetic order with a collinear spin structure, and superconductivity is believed to originate from the FS-driven itinerant spin fluctuations in the SDW ground state.[37] For $Fe_{1+y}Te$, however, the theoretically expected FS nesting and the SDW gap is absent.[3] Moreover, the $A_xFe_{2-y}Se_2$ (A = K, Rb, Cs, etc.) superconductors with strong AFM order even do not exhibit hole pockets.[37] Thereby, the FS nesting scenario seems not necessary or at least not applicable for all the iron-based superconductors. An electronic-structure calculation showed that the bicollinear magnetic order in $Fe_{1+y}Te$ can be effectively described by a frustrated local moment model with J_1, J_2, and J_3 superexchange interactions.[4–6] Even for the iron pnictides, the collinear antiferromagnetism can also be rationalized based on the J_1 and J_2 superexchange interactions.[38] A neutron scattering study suggested the iron pnictides and iron chalcogenides share a common magnetic origin associated with the J_2 magnetic interaction, despite their different magnetic structure.[39] The present $Fe_{1.05}Te{:}O_x$ superconductor has a close T_c to the underdoped Fe_{1+y}(Te,Se/S) and shares a common enhancement of the itinerant character of Fe $3d$ electrons with them. In Fe_{1+y}(Te,Se), the development of superconductivity is accompanied by the gradual suppression of Fe magnetic moment with increasing Se content.[7] Thereby, the enhancement of itinerant character of Fe $3d$ electrons in $Fe_{1.05}Te{:}O_x$ can also be correlated with the suppression of the Fe magnetic moment. Then, spin fluctuations based on the interactions between the irons may be caused to induce the superconductivity. In addition, with reducing the height of Te from the Fe plane, the J_3 decreases and both J_1 and J_2 increase, which pushes up the energy of the AFM ground state.[40] For the iron chalcogenides, the superconducting T_c is found to increase as the chalcogen height is reduced.[41] In the present $Fe_{1.05}Te{:}O_x$, the expanded a parameter and contracted c parameter as result of the inserted oxygen in the Fe-Te layer is compatible with the decrease of Te height, which disfavors the AFM ground state and benefits the superconductivity. This work indicates that superconductivity can be directly induced by suppressing the bicollinear antiferromagnetic order in $Fe_{1.05}Te$ through oxygen incorporation, which suggests that the bicollinear magnetism via superexchange interactions can be considered as the parent phase of the superconductivity.

IV. CONCLUSIONS

In conclusion, we report the discovery of superconductivity in $Fe_{1.05}Te$ single crystals induced by long-time air exposure. TEM investigations imply that the incorporated oxygen partially occupies the interstitial site in the Fe-Te layer, which is supported by the DFT calculation. In contrast to $Fe_{1.05}Te$, a common enhancement of itinerant character of Fe $3d$ electrons is observed for superconducting $Fe_{1.05}Te{:}O_x$ by XPS. Our results show that the bicollinear antiferromagnetism in $Fe_{1+y}Te$ could be considered as the parent phase of superconductivity in the iron chalcogenides.

ACKNOWLEDGMENTS

This research was financially supported by the National Key Basic Research of China Grants No. 2011CBA00111 and No. 2010CB923403, and the National Nature Science Foundation of China Grants No. U1332143, No. 11074258, No. 11204314, No. 11304321, and No. 11274311. Z. T. Zhang was supported by the China Postdoctoral Science Foundation under Grant No. 2013M531535. The calculations were partially performed at the Center for Computational Science CASHIPS.

*Corresponding author: zryang@issp.ac.cn
†Corresponding author: wjlu@issp.ac.cn

[1] F. C. Hsu, J. Y. Luo, K. W. Yeh, T. K. Chen, T. W. Huang, P. M. Wu, Y. C. Lee, Y. L. Huang, Y. Y. Chu, D. C. Yan, and M. K. Wu, Proc. Natl. Acad. Sci. U. S. A. **105**, 14262 (2008).
[2] A. Subedi, L. J. Zhang, D. J. Singh, and M. H. Du, Phys. Rev. B **78**, 134514 (2008).
[3] Y. Xia, D. Qian, L. Wray, D. Hsieh, G. F. Chen, J. L. Luo, N. L. Wang, and M. Z. Hasan, Phys. Rev. Lett. **103**, 037002 (2009).
[4] W. Bao, Y. Qiu, Q. Huang, M. A. Green, P. Zajdel, M. R. Fitzsimmons, M. Zhernenkov, S. Chang, M. H. Fang, B. Qian, E. K. Vehstedt, J. H. Yang, H. M. Pham, L. Spinu, and Z. Q. Mao, Phys. Rev. Lett. **102**, 247001 (2009).
[5] Fengjie Ma, Wei Ji, Jiangping Hu, Zhong-Yi Lu, and Tao Xiang, Phys. Rev. Lett. **102**, 177003 (2009).
[6] C. Fang, B. A. Bernevig, and J. Hu, Europhys. Lett. **86**, 67005 (2009).
[7] T. J. Liu, J. Hu, B. Qian, D. Fobes, Z. Q. Mao, W. Bao, M. Reehuis, S. A. J. Kimber, K. Prokes, S. Matas, D. N. Argyriou, A. Hiess, A. Rotaru, H. Pham, L. Spinu, Y. Qiu, V. Thampy, A. T. Savici, J. A. Rodriguez, and C. Broholm, Nat. Mater. **9**, 716 (2010).
[8] Myung Joon Han and Sergey Y. Savrasov, Phys. Rev. Lett. **103**, 067001 (2009).
[9] G. F. Chen, Z. G. Chen, J. Dong, W. Z. Hu, G. Li, X. D. Zhang, P. Zheng, J. L. Luo, and N. L. Wang, Phys. Rev. B **79**, 140509 (2009).
[10] Y. Han, W. Y. Li, L. X. Cao, X. Y. Wang, B. Xu, B. R. Zhao, Y. Q. Guo, and J. L. Yang, Phys. Rev. Lett. **104**, 017003 (2010).
[11] Y. F. Nie, D. Telesca, J. I. Budnick, B. Sinkovic, and B. O. Wells, Phys. Rev. B **82**, 020508 (2010).
[12] Y. F. Nie, D. Telesca, J. I. Budnick, B. Sinkovic, R. Ramprasad, and B. O. Wells, J. Phys. Chem. Solids **72**, 426 (2011).
[13] D. Telesca, Y. Nie, J. I. Budnick, B. O. Wells, and B. Sinkovic, Phys. Rev. B **85**, 214517 (2012).
[14] Weidong Si, Qing Jie, Lijun Wu, Juan Zhou, Genda Gu, P. D. Johnson, and Qiang Li, Phys. Rev. B **81**, 092506 (2010).
[15] M. Zheng, H. Hu, C. Zhang, B. Mulcahy, J. Zuo, and J. Eckstein, arXiv:1301.4696.
[16] I. K. Dimitrov, W. D. Si, W. Ku, S. J. Han, and J. Jaroszynski, Low Temp. Phys. **39**, 680 (2013).
[17] Y. Mizuguchi, K. Deguchi, S. Tsuda, T. Yamaguchi, and Y. Takano, Europhys. Lett. **90**, 57002 (2010).
[18] C. Zhang, W. Yi, L. Sun, X. J. Chen, R. J. Hemley, H. K. Mao, W. Lu, X. Dong, L. Bai, J. Liu, A. F. Moreira Dos Santos, J. J. Molaison, C. A. Tulk, G. Chen, N. Wang, and Z. Zhao, Phys. Rev. B **80**, 144519 (2009).
[19] Z. T. Zhang, Z. R. Yang, L. Li, L. Pi, S. Tan, and Y. H. Zhang, J. Appl. Phys. **107**, 083903 (2010).
[20] P. E. Blöchl, Phys. Rev. B **50**, 17953 (1994).
[21] M. Torrent, F. Jollet, F. Bottin, G. Zérah, and X. Gonze, Comp. Mater. Sci. **42**, 337 (2008).
[22] X. Gonze, B. Amadon, and E. A. Anglade, Comput. Phys. Commun. **180**, 2582 (2009).
[23] X. Gonze, J. M. Beuken, R. Caracas, F. Detraux, M. Fuchs, G.-M. Rignanese, L. Sindic, M. Verstraete, G. Zerah, F. Jollet, M. Torrent, A. Roy, M. Mikami, P. Ghosez, J.-Y. Raty, and D. Allan, Comp. Mater. Sci. **25**, 478 (2002).
[24] X. Gonze, G.-M. Rignanese, M. Verstrate, J.-M. Beuken, Y. Pouillon, R. Caracas, F. Jollet, M. Torrent, G. Zerah, M. Mikami, P. Ghosez, M. Veithen, J.-Y. Raty, V. Olevano, F. Bruneval, L. Reining, R. Godby, G. Onida, D. R. Hamann, and D. C. Allan,, Z. Kristallogr. **220**, 558 (2005).
[25] J. P. Perdew, K. Burke, and M. Ernzerhof, Phys. Rev. Lett. **77**, 3865 (1996).
[26] H. J. Monkhorst and J. D. Pack, Phys. Rev. B **13**, 5188 (1976).
[27] M. H. Fang, H. M. Pham, B. Qian, T. J. Liu, E. K. Vehstedt, Y. Liu, L. Spinu, and Z. Q. Mao, Phys. Rev. B **78**, 224503 (2008).
[28] Y. Mizuguchi, F. Tomioka, S. Tsuda, T. Yamaguchi, and Y. Takano, Appl. Phys. Lett. **94**, 012503 (2009).
[29] N. R. Werthamer, E. Helfand, and P. C. Hohemberg, Phys. Rev. **147**, 295 (1966).
[30] Hefei Hu, Jian-Min Zuo, Jinsheng Wen, Zhijun Xu, Zhiwei Lin, Qiang Li, Genda Gu, Wan Kyu Park, and Laura H. Greene, New J. Phys. **13**, 053031 (2011).
[31] R. Hu, E. S. Bozin, J. B. Warren, and C. Petrovic, Phys. Rev. B **80**, 214514 (2009).
[32] *Handbook of X-Ray Photoelectron Spectroscopy: A Reference Book of Standard Data For Use In X-Ray Photoelectron Spectroscopy*, edited by C. D. Wagner, W. M. Riggs, L. E. Davis, J. F. Moulder, and G. E. Muilenberg, (Perkin-Elmer, Physical Electronics Division, Eden Prairie, MN, 1979).
[33] V. P. S. Awana, Govind, A. Pal, B. Gahtori, S. D. Kaushik, A. Vajpayee, J. Kumar, and H. Kishan, J. Appl. Phys. **109**, 07E122 (2011).
[34] W. Malaeb, T. Yoshida, T. Kataoka, A. Fujimori, M. Kubota, K. Ono, H. Usui, K. Kuroki, R. Arita, H. Aoki, Y. Kamihara, M. Hirano, and H. Hosono, J. Phys. Soc. Jpn. **77**, 093714 (2008).
[35] E. Z. Kurmaev, J. A. McLeod, A. Buling, N. A. Skorikov, A. Moewes, M. Neumann, M. A. Korotin, Y. A. Izyumov, N. Ni, and P. C. Canfield, Phys. Rev. B **80**, 054508 (2009).
[36] Toru Yamashita and Peter Hayes, Appl. Surf. Sci. **254**, 2441 (2008).
[37] Pengcheng Dai, Jiangping Hu, and Elbio Dagotto, Nat. Phys. **8**, 709 (2012).
[38] Q. Si and E. Abrahams, Phys. Rev. Lett. **101**, 076401 (2008).
[39] O. J. Lipscombe, G. F. Chen, Chen Fang, T. G. Perring, D. L. Abernathy, A. D. Christianson, Takeshi Egami, Nanlin Wang, Jiangping Hu, and Pengcheng Dai, Phys. Rev. Lett. **106**, 057004 (2011).
[40] Chang-Youn Moon and Hyoung Joon Choi, Phys. Rev. Lett. **104**, 057003 (2010).
[41] Y. Mizuguchi and Y. Takano, J. Phys. Soc. Jpn. **79**, 102001 (2010).